Available online at www.sciencedirect.com
ScienceDirect
Trans. Nonferrous Met. Soc. China 25(2015) 504−509
Transactions of Nonferrous Metals Society of China
www.tnmsc.cn

# Preparation and photocatalytic performance of Cu-doped $TiO_2$ nanoparticles

Xi-jia YANG, Shu WANG, Hai-ming SUN, Xiao-bing WANG, Jian-she LIAN

Key Laboratory of Automobile Materials of Ministry of Education, College of Materials Science and Engineering, Jilin University, Changchun 130025, China

Received 1 February 2014; accepted 16 May 2014

**Abstract:** Cu-doped $TiO_2$ nanoparticles with different doping contents from 0 to 2.0% (mole fraction) were synthesized through sol−gel method. X-ray diffraction (XRD), X-ray photoelectron spectroscopy (XPS) and field emission scanning electron microscope (FE-SEM) were used to characterize the crystalline structure, chemical valence states and morphology of $TiO_2$ nanoparticles. UV−Vis absorption spectrum was used to measure the optical absorption property of the samples. The photocatalytic performance of the samples was characterized by degrading 20 mg/L methyl orange under UV−Vis irradiation. The results show that the Cu-doped $TiO_2$ nanoparticles exhibit a significant increase in photocatalytic performance over the pure $TiO_2$ nanoparticles, and the $TiO_2$ nanoparticles doped with 1.0% Cu show the best photocatalytic performance. The improvement in photocatalytic performance is attributed to the enhanced light adsorption in UV−Vis range and the decrease of the recombination rate of photoinduced electron−hole pair of the Cu-doped $TiO_2$ nanoparticles.

**Key words:** $TiO_2$; Cu; nanoparticles; photocatalysis; doping; sol−gel method

## 1 Introduction

Industrial waste water and by-products produced by oxidation are clearly a threat to the ecological environment [1]. How to eliminate such contaminants in water arouses a hot spot in today's scientific research. Photocatalytic degradation of effluents is the simple and environment-friendship technology and has developed rapidly in recent years. $TiO_2$, as a promising semiconductor photocatalyst, has been widely used in wastewater treatment on account of its unique photo-electric properties, high chemical stability, low cost and safety toward both humans and the environment [2−5].

As a wide band semiconductor oxide, the largest wavelength of incident light for $TiO_2$ (anatase) is about 387 nm. Therefore, the photocatalytic efficiency is limited by the inadequate utilization of the sunlight. Meanwhile, the high recombination rate of photogenerated electron ($d^-$)−hole ($h^+$) pair also decreases the photocatalytic activity of $TiO_2$ [6]. In order to optimize the photocatalytic performance of $TiO_2$, different preparation methods [7−10] and a lot of modification methods have been tried [11−14]. The doping of transition metals into $TiO_2$ is an effective way to improve the photocatalytic performance [15−22]. In these studies, Cu, as a kind of transition metal, was found to be an effective dopant for $TiO_2$ to enhance the photocatalytic activity [23].

In the present study, the photocatalytic performance of pure $TiO_2$ and Cu-doped $TiO_2$ nanoparticles which were fabricated via sol−gel method was investigated, and the influence of Cu content on the photocatalytic performance tested by the photocatalytic degradation of methyl orange was discussed. The Cu-doped $TiO_2$ nanoparticles were characterized by X-ray diffraction (XRD), X-ray photoelectron spectroscopy (XPS), field emission scanning electron microscopy (FE-SEM) and UV−Vis absorption spectrum. Meanwhile, the mechanism for the improvement of photocatalytic activity was discussed based on the characterization results.

## 2 Experimental

### 2.1 Preparation method

$TiO_2$ was synthesized through the sol−gel method

**Foundation item:** Project (2010CB631001) supported by the National Basic Research Program of China; Project (50871046) supported by the National Natural Science Foundation of China

**Corresponding author:** Jian-she LIAN; Tel: +86-431-85095876; E-mail: lianjs@jlu.edu.cn

DOI: 10.1016/S1003-6326(15)63631-7

by the hydrolysis of tetrabutyl titanate ($Ti(OC_4H_9)_4$, 10 mL). Tetrabutyl titanate was added dropwise into the mixture solution of 35 mL alcohol and 1 mL acetylacetone. Then, a mixed solution of 10 mL alcohol dissolved with $Cu(NO_3)_2{\cdot}3H_2O$ was added into the vessel dropwise according to the anticipant Cu content (0.5%−2.0%, mole fraction). Finally, the mixture of 2 mL glacial acetic acid, 2 mL deionized water and 20 mL alcohol was droped in the solution. Stirring was held for the whole course and continued for 1 h. After stewing for 24 h, the sol was put in an oven to dry at 80 °C for 48 h to form the gel. The gels were then put in a muffle furnace and calcined at 450 °C for 2 h to acquire the Cu-doped $TiO_2$ powders with different Cu contents from 0.5% to 2.0%.

### 2.2 Characterization

The crystal structure of the powders was analyzed by XRD (Rigaku D/MAX 2500PC), and the XRD patterns were collected in $2\theta$ range from 20° to 80° with a Cu target and a mono-chronometer at 40 kV and 250 mA. FE-SEM (JSM−6700F) was used to study the morphology of the nanoparticles. A tungsten lamp was employed and the acceleration voltage was 10 kV. Before the test, the samples were coated with gold to increase the conductivity. X-ray photoelectric spectrum (XPS) with an ESCALAB Mk II (Vacuum generators) spectrometer using unmonochromatized Al $K_\alpha$ X-ray (240 W) was used to detect complementary information on the chemical combination state of dopant Cu in $TiO_2$.

### 2.3 Measurement of photodecolorization activity

The photocatalytic performance of the Cu-doped $TiO_2$ nanoparticles was tested by degrading 20 mg/L methyl orange which was carried out in a home-built reactor. A 250 W high-pressure mercury lamp with light wavelength from 350 nm to 450 nm was used as a light source. In each run, after the mixture of 10 mg Cu/$TiO_2$ catalyst and 30 mL methyl orange solution of 20 mg/L was reposed at dark for 10 min, the light was turned on to initiate the degradation process. A UV−6100(PC) spectrometer made by MeiPuda Company was used to determine the concentration of methyl orange solution before and after the photocatalytic degradation every 20 min once. The UV–Vis spectrophotometer was also used to measure the absorbance spectrum of the $TiO_2$ nanoparticles.

## 3 Results and discussion

### 3.1 Structure analysis

The XRD patterns of Cu-doped $TiO_2$ and $TiO_2$ nanoparticles are shown in Fig. 1. The diffraction peaks were indexed to (101), (103), (004), (112), (200), (105), (211), (204), (116), (220) and (215) planes of anatase

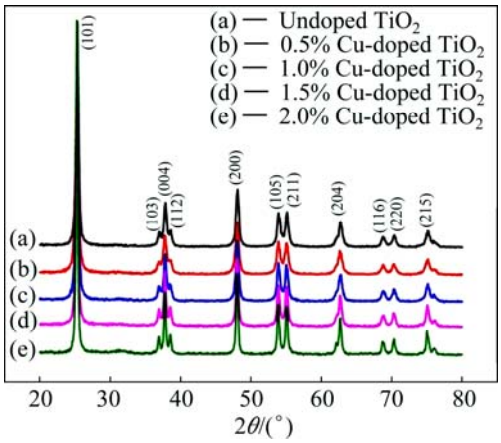


**Fig. 1** XRD patterns of $TiO_2$ and Cu-doped $TiO_2$ nanoparticles with different Cu contents from 0.5% to 2.0%

phase of $TiO_2$ (JCPDS No. 21−1272), and no other Cu or Cu relative peaks were observed, implying that Cu was doped into $TiO_2$ lattice. The crystallite size of the samples was calculated from full-width at half-maximum (FWHM) of the (101) peak of anatase $TiO_2$ by the Debye-Sherrer equation:

$$d=k\lambda/(\beta\cos\theta) \quad (1)$$

where $d$ represents the crystallite size; $\lambda$ represents the wavelength of incident X-ray; $\beta$ is the FWHM of diffraction peak; $\theta$ represents the scattering angle. All the XRD patterns show the increased FWHM values, indicating that the synthesized particles are in nanocrystalline range. For example, the calculated grain size of 1% Cu-doped $TiO_2$ particles is 24.73 nm. Real particle size can be directly revealed by FE-SEM observation. FE-SEM micrographs of pure $TiO_2$ and 1.0% Cu-doped $TiO_2$ are shown in Figs. 2(a) and (b), respectively. The particles are quite uniform and show round or polyhedron shape with particle size in the range of 40−70 nm for $TiO_2$ in Fig. 2(a) and 30−45 nm for 1.0% Cu-doped $TiO_2$ in Fig. 2(b). That is, a decrease in particle size due to Cu doping is observed. When $Cu^{2+}$ ions doped into $TiO_2$ lattice, they like to dwell in grain boundary regions or on the surface of particles to inhibit the growth of $TiO_2$ crystals [24].

Quantitative XPS analysis of $TiO_2$ and 1.0% Cu-doped $TiO_2$ samples was performed. Figure 3(a) shows the Cu 2p spectrum of 1.0% Cu-doped $TiO_2$. There are two characteristic peaks located at 932.9 and 953.2 eV, which are corresponding to the binding energies of Cu $2p_{3/2}$ and Cu $2p_{1/2}$, respectively, i.e., Cu exists as $Cu^{2+}$ ions in $TiO_2$ [25]. Figure 3(b) illustrates the Ti 2p spectra of $TiO_2$ and 1.0% Cu-doped $TiO_2$. For $TiO_2$, the peaks located at 458.1 and 464.0 eV are Ti $2p_{3/2}$ and Ti $2p_{1/2}$ states, respectively, while for 1.0% Cu-doped $TiO_2$, the binding energies of Ti $2p_{3/2}$ and Ti $2p_{1/2}$ states

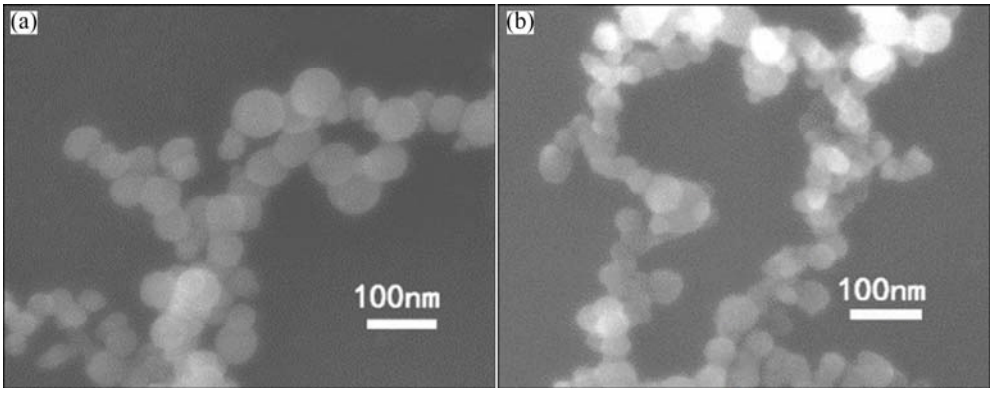


**Fig. 2** FE-SEM images of $TiO_2$ (a) and 1.0% Cu-doped $TiO_2$ (b) nanoparticles

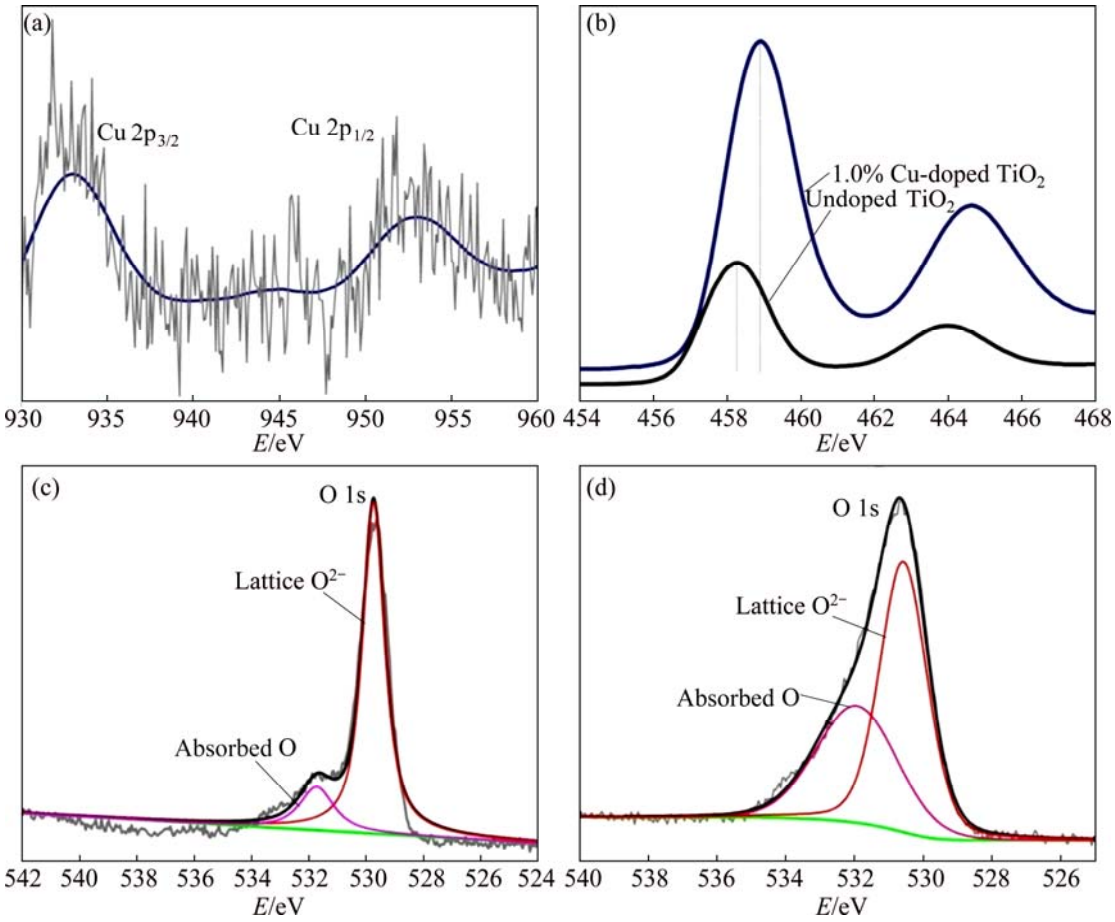


**Fig. 3** XPS spectra of Cu 2p for 1.0% Cu-doped $TiO_2$ (a), Ti 2p for $TiO_2$ and 1.0% Cu-doped $TiO_2$ (b), O 1s for $TiO_2$ (c) and O 1s for 1.0% Cu-doped $TiO_2$ (d)

increase slightly to 458.4 and 464.4 eV, respectively, which may also reflect that $Cu^{2+}$ ions have been doped into $TiO_2$ lattice.

The XPS spectra of O 1s for $TiO_2$ and 1.0% Cu-doped $TiO_2$ are shown in Figs. 3(c) and (d), respectively. The spectra are fitted with the non-linear least square fit program using Gauss−Lorentzian peak shapes, and two O 1s peaks are observed, which are attributed to the lattice oxygen ((529.9±0.1) eV) and the absorbed oxygen ((531.8±0.1) eV) in $TiO_2$. The latter reflects not only the absorbed oxygen but also the adsorbed $H_2O$ or hydroxyl oxygen (OH) groups on the surface [26]. There is more adsorbed oxygen ($H_2O$ or OH groups) on the surfaces of 1.0% Cu-doped $TiO_2$ compared with the undoped $TiO_2$ nanoparticles. When introducing Cu into $TiO_2$, $Cu^{2+}$ ion should substitute $Ti^{4+}$ in $TiO_2$ lattice, which means that O—Ti—O turns to Cu—O, resulting in the increase of oxygen vacancies. The increased adsorbed oxygen ($H_2O$ or OH groups) on the surface should balance the increased oxygen vacancies in $TiO_2$ lattices [27].

### 3.2 Optical performance Cu-doped $TiO_2$ nanoparticles

The UV−Vis absorbance spectra of $TiO_2$ nanoparticles with different Cu doping contents and undoped $TiO_2$ are illustrated in Fig. 4(a). Compared with the absorbance spectrum of undoped $TiO_2$ nanoparticles, Cu-doped $TiO_2$ nanoparticles have a higher light harvest performance reflected by not only the widening of its UV absorbance peak, but also the evident enhancement of light absorbance covering the whole visible range. The red shift of the band gap can be obtained by the plot of $(Ah\nu)^2$ vs $h\nu$ ($E_g$) in Fig. 4(b) ($A$ is the absorbance; $h$ is the Planck constant; $\nu$ is the frequency of incident light), which reveals that the band gap shifts from 3.28 eV for the undoped $TiO_2$ to 3.02−3.17 eV for the Cu-doped $TiO_2$.

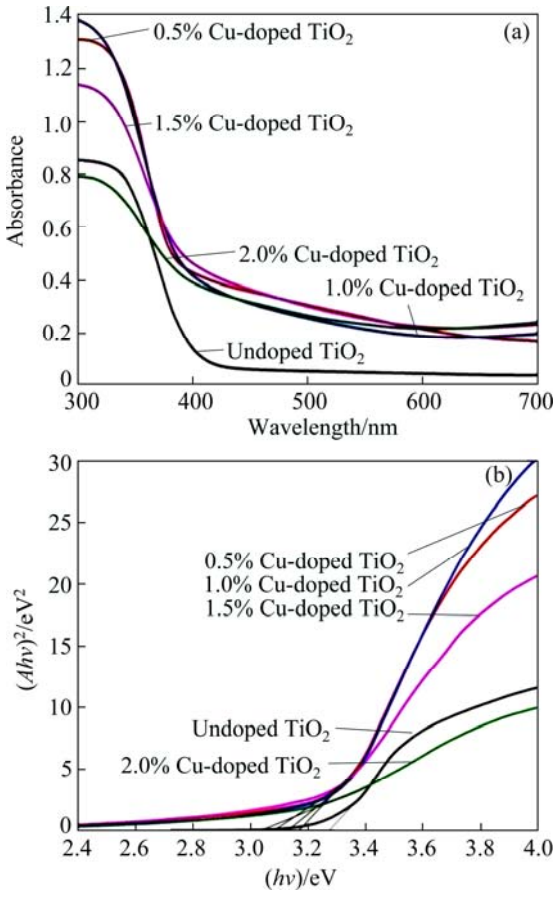


**Fig. 4** UV−Vis absorption spectra of $TiO_2$ and Cu-doped $TiO_2$ nanoparticles with different Cu contents (a) and $(Ah\nu)^2$ vs $h\nu$ curves from absorption spectra to get band gap values (b)

### 3.3 Photocatalytic degradation of methyl orange

Figure 5 shows the photocatalytic activity of Cu-doped $TiO_2$ with different Cu contents and undoped $TiO_2$ on the degradation of 20 mg/L methyl orange. It is seen that the Cu-doped $TiO_2$ with Cu content of 0.5%−1.5% shows improved photocatalytic performance, and 1.0% Cu-doped $TiO_2$ shows the best photocatalytic performance among them. When the content of Cu doping reaches 2.0%, the photocatalytic performance decreases to the level similar to that of undoped $TiO_2$.

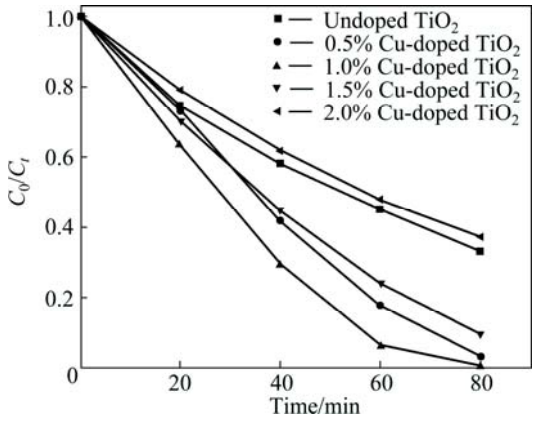


**Fig. 5** Photodegradation of methyl orange under using Cu-doped $TiO_2$ with different Cu contents and undoped $TiO_2$ as catalyzers

The increased photocatalytic performance of Cu-doped $TiO_2$ can be attributed to the following reasons. Firstly, as shown in Fig. 4 (a), the absorbance spectra of Cu-doped $TiO_2$ exhibit the enhanced light harvest in both UV and visible light regions, which enable much more light energy to be utilized for photocatalysis. Secondly, Cu species (CuO/$Cu_2O$/metallic Cu) have smaller band gap and higher work function than bare $TiO_2$, so the electron can transfer from the conduction band of $TiO_2$ to metallic copper ion. This results in the formation of Schottky barrier in the metal−semiconductor contact region, which facilitates the charge separation, and hence enhances the photocatalytic performance of $TiO_2$. The inducing impurity energy level by doping Cu also plays an important role in the effective separation of photoinduced electron−hole pair. Since the valence of $Cu^{2+}$ ion is less than that of $Ti^{4+}$, doping of Cu will induce oxygen vacancies, which act as the active sites for water dissociation on the surface of $TiO_2$, and can also capture the holes to restrain the recombination of hole−electron pairs. Thus, the photocatalytic performance of $TiO_2$ is enhanced [28].

However, when much more $Cu^{2+}$ ions are doped, they can trap the photoinduced electrons to form $Cu^+$ ions. Since $\varphi^0(Cu^{2+}/Cu^+)$=0.16 V (vs NHE), while $\varphi^0(Cu^{2+}/Cu^+)$=0.25 V (vs NHE) [29], the formed $Cu^+$ ions can capture the photoinduced holes and generate $Cu^{2+}$. Thus, a short-circuiting forms and both photoinduced electron and hole are consumed. Consequently, the photocatalytic activity is reduced. Therefore, there is an optimum Cu content (1.0% in this study) at which the Cu-doped $TiO_2$ can effectively separate the photoinduced electron−hole pair and perform the best photocatalytic performance.

## 4 Conclusions

1) Cu exists in the form of $Cu^{2+}$ ions in $TiO_2$ lattice, which induce more oxygen vacancies and trap much more absorbed oxygen (or $H_2O$ or OH groups) on the surface of $TiO_2$ nanoparticles, as testified by the XPS spectrum of O 1s peaks.

2) Cu-doped $TiO_2$ shows an enhanced light harvest in both UV and visible light regions, which is beneficial to its photocatalytic performance.

3) With an appropriate content of Cu (0.5%−1.5%), the Cu-doped $TiO_2$ nanoparticles exhibit the improved photocatalytic performance in photo degradation of methyl orange, and the best performance is achieved at Cu doping content of 1.0%.

## References

[1] ZOLLINGER H. Color chemistry: Synthesis, properties and applications of organic dyes and pigments [M]. Zurich: Wiley-VCH, 1991: 1−593.

[2] KONSTANTINOU I K, ALBANIS T A. $TiO_2$-assisted photocatalytic degradation of azo dyes in aqueous solution: Kinetic and mechanistic investigations: A review [J]. Applied Catalysis B: Environmental, 2004, 49(1): 1−14.

[3] LI Xiang, XIONG Rong-chun, WEI Gang. Preparation and photocatalytic activity of nanoglued Sn-doped $TiO_2$ [J]. Journal of Hazardous Materials, 2009, 164(2−3): 587−591.

[4] ZHU Xiang-dong, ZHOU Dong-mei, CANG Long, WANG Yu-jun. $TiO_2$ photocatalytic degradation of 4-chlorobiphenyl as affected by solvents and surfactants [J]. Journal of Soils and Sediments, 2012, 12(3): 376−385.

[5] LI Ming, TANG Pei-song, HONG Zhang-lian, WANG Min-quan. High efficient surface−complex-assisted photodegradation of phenolic compounds in single anatase titania under visible-light [J]. Colloids and Surfaces A: Physicochemical and Engineering Aspects, 2008, 318(1−3): 285−290.

[6] LINSEBIGLER A L, LU G Q, YATES J T. Photocatalysis on $TiO_2$ surfaces: Principles, mechanisms, and selected results [J]. Chemical Reviews, 1995, 95(3): 735−758.

[7] GHODSI F E, TEPEHAN F Z, TEPEHAN G G. Study of time effect on the optical properties of spin-coated $CeO_2$–$TiO_2$ thin films [J]. Solar Energy Materials & Solar Cells, 2001, 68(3−4): 355−364.

[8] RAMPAUL A, PARKIN I P, O'NEILL S A, DESOUZA J, MILLS A, ELLIOTT N. Titania and tungsten doped titania thin films on glass: Active photocatalysts [J]. Polyhedron, 2003, 22(1): 35−44.

[9] ALMQUIST C B, BISWAS P. Role of synthesis method and particle size of nanostructured $TiO_2$ on its photoactivity [J]. Journal of Catalysis, 2002, 212(2): 145−156.

[10] GRACIA F, HOLGADO J, CONTRERAS L, GIRARDEAU T, GONZALEZ-ELIPE A R. Optical and crystallisation behaviour of $TiO_2$ and V/$TiO_2$ thin films prepared by plasma and ion beam assisted methods [J]. Thin Solid Films, 2003, 429(1−2): 84−90.

[11] DIWALD O, THOMPSON T L, ZUBKOV T, GORALSKI E G, WALCK S D, YATES J T Jr. Photochemical activity of nitrogen-doped rutile $TiO_2$(110) in visible light [J]. The Journal of Physical Chemistry B: Chemical, 2004, 108(19): 6004−6008.

[12] SONAWANE R S, KALE B B, DONGARE M K. Preparation and photo-catalytic activity of Fe/$TiO_2$ thin films prepared by sol–gel dip coating [J]. Materials Chemistry and Physics, 2004, 85(1): 52−57.

[13] OH J H, LEE H, KIM D, SEONG T Y. Effect of Ag nanoparticle size on the plasmonic photocatalytic properties of $TiO_2$ thin films [J]. Surface & Coatings Technology, 2011, 206(1): 185−189.

[14] NOGAWA T, ISOBE T, MATSUSHITA S, NAKAJIMA A. Preparation and visible-light photocatalytic activity of Au- and Cu-modified $TiO_2$ powders [J]. Materials Letters, 2012, 82(1): 174−177.

[15] ZHU Jie-fang, ZHENG Wei, HE Bin, ZHANG Jin-long, ANPO M. Characterization of Fe−$TiO_2$ photocatalysts synthesized by hydrothermal method and their photocatalytic reactivity for photodegradation of XRG dye diluted in water [J]. Journal of Molecular Catalysis A: Chemical, 2004, 216(1): 35−43.

[16] PAWAR M J, NIMBALKAR V B. Synthesis and phenol degradation activity of Zn and Cr doped $TiO_2$ nanoparticals [J]. Research Journal of Chemical Sciences, 2012, 2(1): 32−37.

[17] HIRAKAWA T, KAMAT P V. Charge separation and catalytic activity of Ag@$TiO_2$ core-shell composite clusters under UV-irradiation [J]. Journal of the American Chemical Society, 2005, 127(11): 3928−3934.

[18] LI Jun-qi, WANG De-fang, LIU Hui, ZHU Zhen-feng. Multilayered Mo-doped $TiO_2$ nanofibers and enhanced photocatalytic activity [J]. Materials and Manufacturing Processes, 2012, 27(6): 631−635.

[19] BINGHAM S, DAOUD W A. Recent advances in making nano-sized $TiO_2$ visible-light active through rare-earth metal doping [J]. Journal of Materials Chemistry, 2011, 21(1): 2041−2050.

[20] WU N L, LEE M S. Enhanced $TiO_2$ photocatalysis by Cu in hydrogen production from aqueous methanol solution [J]. International Journal of Hydrogen Energy, 2004, 29(15): 1601−1605.

[21] YU H, IRIE H, HASHIMOTO K. Conduction band energy level control of titanium dioxide: Toward an efficient visible-light-sensitive photocatalyst [J]. Journal of the American Chemical Society, 2010, 132(20): 6898−6899.

[22] ARAI T, YANAGIDA M, KONISHI Y, IKURA A, IWASAKI Y, SUGIHARA H, SAYAMA K. The enhancement of $WO_3$-catalyzed photodegradation of organic substances utilizing the redox cycle of copper ions [J]. Applied Catalysis B: Environmental, 2008, 84(1−2): 42−47.

[23] SRINIVAS B, SHUBHAMANGALA B, LALITHA K, REDDY P A K, KUMARI1 V D, de SUBRAHMANYAM M B R. Photocatalytic reduction of $CO_2$ over Cu−$TiO_2$/molecular sieve 5A composite [J]. Photochemistry and Photobiology, 2011, 87(5): 995−1001.

[24] ZHANG Wen-jie, LI Ying, ZHU Sheng-long, WANG Fu-hui. Copper doping in titanium oxide catalyst film prepared by DC reactive magnetron sputtering [J]. Catalysis Today, 2004, 93−95: 589−594.

[25] HUSSAIN Z, SALIM M A, KHAN M A, KHAWAJA E E. X-ray photoelectron and Auger spectroscopy study of copper−sodium−germanate glasses [J]. Journal of Non-Crystalline Solids, 1989, 110(1): 44−52.

[26] WANG Shu, BAI Li-na, SUN Hai-ming, JIANG Qing, LIAN Jian-she. Structure and photocatalytic property of Mo-doped $TiO_2$ nanoparticles [J]. Powder Technology, 2013, 244: 9−15.

[27] WANG Shu, LIAN Jian-she, ZHENG Wei-tao, JIANG Qing. Photocatalytic property of Fe doped anatase and rutile $TiO_2$ nanocrystal particles prepared by sol–gel technique [J]. Applied Surface Science, 2012, 263(15): 260−265.

[28] SCHAUB R, THOSTRUP P, LOPEZ N, LAEGSGAARD E, STENSGAARD I, NØRSKOV J K, BESENBACHER F. Oxygen vacancies as active sites for water dissociation on rutile $TiO_2$(110) [J]. Physical Review Letters, 2001, 87(26): 266801.

[29] XIONG Zhi-gang, ZHANG Li-li, ZHAO Xiu-song. Visible-light-induced dye degradation over copper-modified reduced graphene oxide [J]. Chemistry—A European Journal, 2011, 17(8): 2428−2434.

# 掺铜二氧化钛纳米颗粒的制备及其催化性能

杨希佳，王 姝，孙海明，王晓兵，连建设

吉林大学 材料科学与工程学院 汽车材料教育部重点实验室，长春 130025

**摘 要**：采用溶胶−凝胶法制备掺铜量为 0~2.0%(摩尔分数)的二氧化钛纳米颗粒。应用 X 射线衍射(XRD)、X 射线光电子能谱(XPS)和场发射电子显微镜(FE-SEM)技术对二氧化钛纳米颗粒的晶体结构、化学价态和形貌进行表征。样品的光学吸收性能用紫外−可见吸收光谱进行表征；其光催化性能通过在紫外−可见光照射下分解 20 mg/L 甲基橙溶液进行表征。结果表明，掺铜二氧化钛纳米颗粒具有比纯二氧化钛更优的光催化性能，尤其是铜掺杂量为 1.0%的二氧化钛 $TiO_2$ 纳米颗粒具有最好的光催化性能。铜掺杂能提高二氧化钛在紫外−可见光区对光的吸收、减小电子−空穴对的复合，因此，铜掺杂使二氧化钛的光催化性能得到提高。

**关键词**：二氧化钛；铜；纳米颗粒；光催化；掺杂；溶胶−凝胶

**(Edited by Wei-ping CHEN)**